Rheological and Topological Characterizations of Electron Beam Irradiation Prepared Long-Chain Branched Polylactic Acid

Yongbin Wang,[1] Liang Yang,[1] Yanhua Niu,[1] Zhigang Wang,[1,2] Jun Zhang,[1] Fengyuan Yu,[3] Hongbin Zhang[3]

[1]*CAS Key Laboratory of Engineering Plastics, Beijing National Laboratory for Molecular Sciences, Institute of Chemistry, Chinese Academy of Sciences, Beijing 100190, People's Republic of China*
[2]*CAS Key Laboratory of Soft Matter Chemistry, Department of Polymer Science and Engineering, Hefei National Laboratory for Physical Sciences at the Microscale, University of Science and Technology of China, Hefei, Anhui Province 230026, People's Republic of China*
[3]*Advanced Rheology Institute, Department of Polymer Science and Engineering, Shanghai Jiao Tong University, Shanghai 200240, People's Republic of China*

Received 22 December 2010; accepted 31 January 2011
DOI 10.1002/app.34276
Published online 10 June 2011 in Wiley Online Library (wileyonlinelibrary.com).

ABSTRACT: In this study, a series of linear- and long-chain branched polylactic acid (PLA) samples was prepared by electron beam irradiation without or with addition of a trifunctional monomer, trimethylolpropane triacrylate (TMPTA). The chain structures of the PLA samples were characterized by size-exclusion chromatography coupled with a light scattering detector (SEC-MALLS) and shear and extensional rheology. PLA tends to degrade while keeps linear structures with increasing irradiation dose and without addition of TMPTA, as evidenced by decreased molecular mass M_w and reductions of storage modulus G′ and the zero shear viscosity η_0. Long-chain branched PLA samples were successfully prepared with irradiation and addition of TMPTA, which shows prominent higher η_0 and apparent flow activation energy, longer characteristic relaxation time τ, and pronounced strain-hardening behaviors. With increasing amount of TMPTA, M_w dependences of η_0 and the root mean square radius of gyration R_g obviously deviate from the scaling relation of linear PLA samples, which strongly indicates the increased long-chain branching degree for the branched PLA samples. © 2011 Wiley Periodicals, Inc. J Appl Polym Sci 122: 1857–1865, 2011

Key words: rheology; long-chain branched; polylactic acid

INTRODUCTION

Polylactic acid (PLA) has recently gained utmost attention because of its biodegradable and biocompatible nature, which makes it valuable in biomedical and pharmaceutical applications.[1,2] Considering its highly versatile properties, PLA is expected to be one of the most competitive and promising candidates to substitute some petroleum-based polymers, i.e., polystyrene and poly(ethylene terephthalate) in future applications.[3,4] However, some inherent shortcomings including shear-insensitive melt viscosity, poor melt strength of linear PLA, and brittleness of PLA productions impede its development for large-scale commercial uses. Therefore, modification of linear PLA has become an active research area nowadays.

Through introduction of long-chain branching (LCB), the rheological behaviors, processability, crystallization kinetics, and mechanical properties of polyolefins can be largely improved while their essential characters remain.[5,6] LCB is generally defined as the branch with a molecular mass at least greater than the entanglement molecular mass, M_e, which is around 1 kg/mol for polyethylene[7] and 4 kg/mol for PLA.[8] Besides directly incorporated during synthesis,[9] LCB can be conveniently introduced by high-energy irradiation,[10,11] during which the LCB level can be approximately controlled by changing irradiation dose. For polymers with relatively low LCB levels, detection and determination of such low LCB levels have long been a controversy because of inherent shortcomings of traditional measurements, i.e., NMR, FTIR, and SEC-MALLS. Rheology is more sensitive on detection of LCB than other measurements; however, it always entwines with molecular mass distribution.[12,13] Therefore,

Correspondence to: Y. Niu (yhniu@iccas.ac.cn) or Z. Wang (zgwang2@ustc.edu.cn).
Contract grant sponsor: The Startup Fund, University of Science and Technology of China.
Contract grant sponsor: The National Science Foundation of China; contract grant number: 50803073.
Contract grant sponsor: The National Science Foundation of China; contract grant number: 51073145.

evidences about LCB in polymers were usually investigated through combination of the aforementioned two or three methods.[11–15] Compared with other traditional methods, rheology has been proven a more sensitive tool to detect a low amount of LCB on the basis of the relation between rheological quantities and topologies deduced from well-defined long-chain branched polymers.[16,17] Up to now, a vast amount of literature has accumulated on detection and determination of LCB levels of long-chain branched polyolefins (both the model polymers and irradiation-induced LCB ones). Some general features have been extracted from the extensive investigations on long-chain branched polymers, especially on polyolefins. For example, compared with the linear chains with the same molecular mass, polyethylene with a low amount of LCB shows relatively higher Newtonian viscosity, lower shear rate values of shear thinning, higher activation flow energy, broader relaxation spectrum, and enhanced elasticity.[12,17] In an extensional flow, a prominent strain-hardening behavior is another signature of LCB.[11] Through the so-called van Gurp–Palmen analysis,[18] the branching architectures, i.e., combs, stars, and dendrites, can be distinguished, and the lengths and amount of branches can be easily interpreted.[14,16] Combining with the molecular masses determined by laser light scattering, rheological measurements can provide new insights into the relation between viscoelasticity and topology of the branched structures including quantitative determination of the LCB level.[11,14,19,20]

With the commercialization of PLA, its rheological properties are of increasing importance. Several careful studies paid close attention to the degradation effects. For example, Cooper-White and Mackay[21] reported that the plateau modulus, G_N^0, of PLA was about 5.5×10^5 Pa, and the scaling exponent between the zero shear viscosity, η_0, and molecular mass was 4.0, which in the report of Dorgan et al.[8] were presented as 5.0×10^5 Pa and 3.4, respectively. Dorgan and coworkers[22] also found a strong strain-hardening behavior for linear PLA with high L-content and ascribed this uncommon phenomenon to the high molecular mass tail, where the rate of deformation considerably exceeds the rate of molecular relaxation. They also demonstrated in another study[8] that the molecular parameters, i.e., the packing length of 2.51 Å, tube diameter of 47.7 Å, and characteristic ratio of 6.5 ± 0.9, for linear PLAs with various L-contents were independent of their stereoisomeric composition. For both the well-defined star-shaped PLAs and peroxide branched commercial grade PLAs,[23,24] the enhancement of η_0 and more serious shear thinning were observed. The exponential dependence of η_0 and the arm length for the well-defined star-shaped PLAs were attributed to the arm retraction. In the work of Yamane et al.,[25] the LCB of PLLA was introduced through formation of the stereocomplex by adding a low amount of poly (D-lactic acid) (PDLA). Strong strain-hardening behavior was observed in the case that the molecular mass of PDLA is sufficiently high.

In this study, we mainly aim at modifying the rheological properties and processability of PLA by introducing LCB through a facile method, i.e., the electron beam irradiation method. By changing the post-treatment conditions, various PLA chain structures can be obtained, which show a great significance from the application viewpoint. With addition of a trifunctional monomer, trimethylolpropane triacrylate (TMPTA), a series of long-chain branched PLA samples were prepared. SEC-MALLS, shear, and extensional rheology were combined to investigate the influences of irradiation condition on the chain architecture diversity and further confirm the formed LCB structures.

EXPERIMENTAL

Materials and sample preparation

Linear PLA (PLA2002D, purchased from the Natureworks China/Hong Kong, Shanghai, China) had number average molecular mass, M_n, of 8.6×10^4 g mol^{-1}, mass average molecular mass, M_w, of 1.14×10^5 g mol^{-1}, room temperature density of 1.24 g cm^{-3}, and a melt flow index of 4.8 g/10 min (190°C, 2.16 kg). A trifunctional monomer, trimethylolpropane triacrylate (TMPTA, purity of 99%), was supplied by Tianjin Tianjiao Chemical Company, Tianjin, China. TMPTA was first dissolved in acetone of 20 mL to form a solution, and then the solution was gradually added into PLA granules of 30 g with stirring. Acetone was then allowed to volatilize completely. The obtained PLA granules (mixed with TMPTA) were melt-processed at 160°C with a rotation speed of 20 rpm and a mixing time of 6 min in a Haake Rheocord 90 mixer.

Irradiation processes were performed by using 12-MeV electrons emitted from an electron beam accelerator BEV-5 (China Institute of Atomic Energy, Beijing, China). After irradiation, the samples were annealed at 80°C for 30 min allowing sufficient migrations of chain fragments to form branched chain structures. Then, the residual radicals were deactivated by annealing at 100°C for 30 min. The sample codes are listed in Table I in which PLA0–4 represents the samples irradiated in vacuum condition with different irradiation doses, and LCB-PLA1–4 represents the samples irradiated in vacuum condition with a fixed irradiation dose of 5 kGy and addition of different amounts of TMPTA.

The formation mechanisms of linear, long-chain branched or crosslinked structures for PLA during

TABLE I
Experimental Formulae for Preparation of PLA Samples

Sample code	PLA (g)	TMPTA amount (wt %)	Irradiation dose (kGy)
PLA0	30	0	0
PLA1	30	0	5
PLA2	30	0	10
PLA3	30	0	30
PLA4	30	0	50
LCB-PLA1	30	0.2	5
LCB-PLA2	30	0.4	5
LCB-PLA3	30	0.6	5
LCB-PLA4	30	0.8	5

electron beam irradiation with addition of TMPTA are schematically shown in Figure 1. During electron beam irradiation, free radicals can be generated at the tertiary hydrogen atom positions on the linear PLA backbone chains, and the random chain scission leads to degradation; however, the chain topology remains linear. Addition of TMPTA as a crosslink reagent can combine the free macroradicals to form the LCB structure. Since the chain scission and macroradical combination are regarded as two competitive procedures, adding a low amount of TMPTA can minimize degradation and effectively enhance chain combination; however, the crosslinked structure forms eventually with loading of much more amount of TMPTA.

To eliminate possible crosslinked components or small gel particles formed in the irradiation processes, LCB-PLA1–4 samples were extracted in chloroform at room temperature for 24 h, and then the soluble portions were precipitated into a large quantity of cold methanol. The precipitated PLA samples were dried and melt-pressed into disk-like sheets for further rheological and SEC-MALLS measurements. The melting temperatures of both linear PLA and LCB-PLA were $\sim$ 153°C as determined by differential scanning calorimetry (DSC TA-Q200) at a heating rate of 10°C/min.

Molecular characterization

The molecular mass characterizations of the PLA samples were carried out by using the Perkin–Elmer size exclusion chromatography coupled with a DAWN EOS multiangle laser light scattering detector (SEC-MALLS) and a refractive index detector. The measurements were performed with a flow rate of 1.0 mL/min for the eluent of tetrahydrofuran (THF) at 30°C. The molecular mass parameters (M_w, M_n, and M_w/M_n) were calculated from the SEC-MALLS data using the commercial software ASTRA 4.73 (Wyatt Technology, Santa Barbara, CA, USA). The obtained values of molecular mass and molecular mass distribution for the PLA samples are listed in Table II. The slight fluctuation of molecular mass distribution for PLA0–4 samples may arise due to

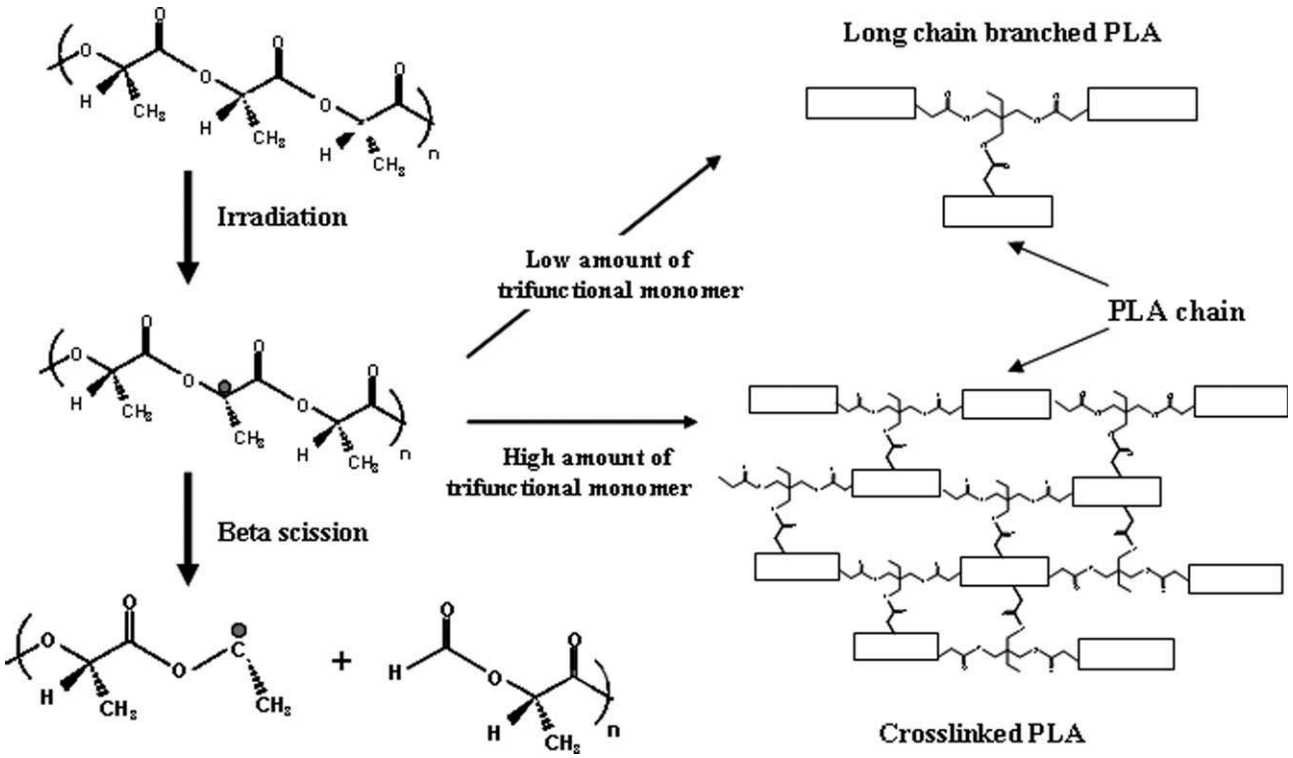

Figure 1 Schematic of degradation and formations of long-chain branched and crosslinked structures for PLA under electron beam irradiation with addition of different amounts of trifunctional monomer.

TABLE II
Molecular Masses and Distributions of PLA Samples from SEC-MALLS Measurements

Sample code	M_n ($\times 10^5$ g/mol)	M_w ($\times 10^5$ g/mol)	M_w/M_n
PLA0	0.86	1.14	1.32
PLA1	0.63	1.03	1.63
PLA2	0.59	0.86	1.46
PLA3	0.52	0.74	1.43
PLA4	0.42	0.61	1.35
LCB-PLA1	0.71	1.11	1.57
LCB-PLA2	1.26	2.14	1.70
LCB-PLA3	1.67	2.89	2.09

the irradiation method, since it provides less well-defined chain structures than a synthesis method. Note that LCB-PLA4 could not be dissolved in THF at room temperature, and its molecular characterization could not be done.

Shear flow rheological measurements

A stress-controlled rheometer (TA-AR2000, TA Instruments, New Castle, DE , USA) with a parallel-plate geometry (diameter of 25 mm) was used for shear rheological measurements. Disk-like PLA samples with thickness of 1 mm and diameter of 25 mm were prepared by melt-pressing at 170°C for 5 min. Before rheological measurements, the samples were dried in a vacuum oven at 60°C for 12 h to remove moistures.

Small amplitude oscillatory frequency sweeps covering a frequency range from 0.01 to 100 rad/s were performed at 160°C with a fixed strain of 2.0% (well falling within the linear viscoelastic region). Steady shear measurements with a shear rate range from 0.002 to 10 s^{-1} were performed at 160°C for all the samples. To confirm the thermal stability of PLA samples during the rheological measurements, dynamic time sweeps were carried out for PLA0 sample at 160°C with two fixed frequencies of 1 and 0.05 rad/s. Although PLA might undergo degradation when exposed to an elevated temperature,[4,22] the time sweep data shown in Figure 2 indicate that within a reasonable error limit (±10%), the PLA sample shows sufficient thermal stability during the 2-h rheological measurements, which ensures the reliability of our rheological results.

Uniaxial extensional flow rheological measurements

Uniaxial extensional flow rheological measurements were performed on an ARES strain-controlled rheometer equipped with an extensional viscosity fixture. PLA samples were prepared by melt-pressing at 170°C into sheets with a size of 0.7 mm × 10 mm × 18 mm. Extensional stress growths were measured at 160°C with strain rates varying from 0.005 to 10 s^{-1}. A prestretch procedure with a stretch rate of 0.05 s^{-1} and a stretch time of 20 s was applied before measurements to compensate the thermal expansion during extension. All the measurements were preformed in a nitrogen atmosphere.

RESULTS AND DISCUSSION

Small amplitude oscillatory frequency sweep measurements

Figure 3 shows the effect of irradiation dose on shear rheological properties of PLA (from PLA0 to PLA4) at 160°C. G' decreases proportionally with increasing irradiation dose (within the whole frequency range), and the slopes at the low frequencies are close to 2 [Fig. 3(a)]. According to the linear viscoelastic theory, it can be deduced that the irradiated PLA0 to PLA4 samples have linear chain structures with narrow molecular mass distributions when treated only by using different irradiation doses in vacuum condition. Figure 3(b) shows the frequency dependences of complex viscosity $|\eta^*|$ for PLA0 to PLA4 samples with different irradiation doses. As expected, $|\eta^*|$ decreases with increasing irradiation dose indicating the reduced molecular mass, which is consistent with the SEC-MALLS results shown in Table II.

Much different from the linear PLA samples (PLA0–4) prepared only by changing irradiation dose, rheological properties of PLA samples (LCB-PLA1–4) prepared with addition of various amounts of TMPTA are more complex. Figure 4(a) shows frequency dependences of G' for LCB-PLA1–4 samples at 160°C with the curve of PLA0 sample as a reference. As the amount of TMPTA increases, G' values in the low frequency region are pronouncedly

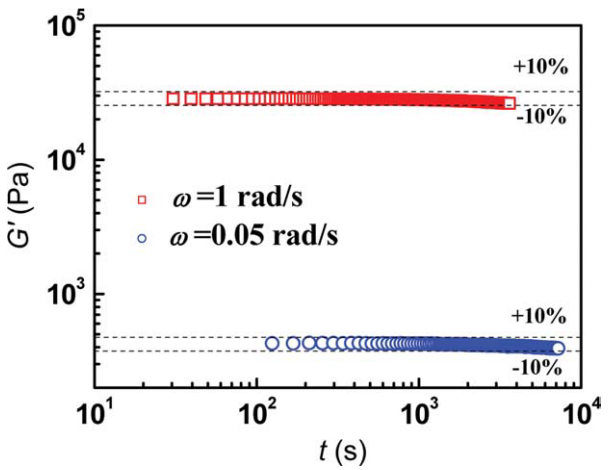

Figure 2 Variation of the storage modulus G' during the time sweeps for PLA0 sample at 160°C with the fixed frequencies of 1 and 0.05 rad/s. [Color figure can be viewed in the online issue, which is available at wileyonlinelibrary.com.]

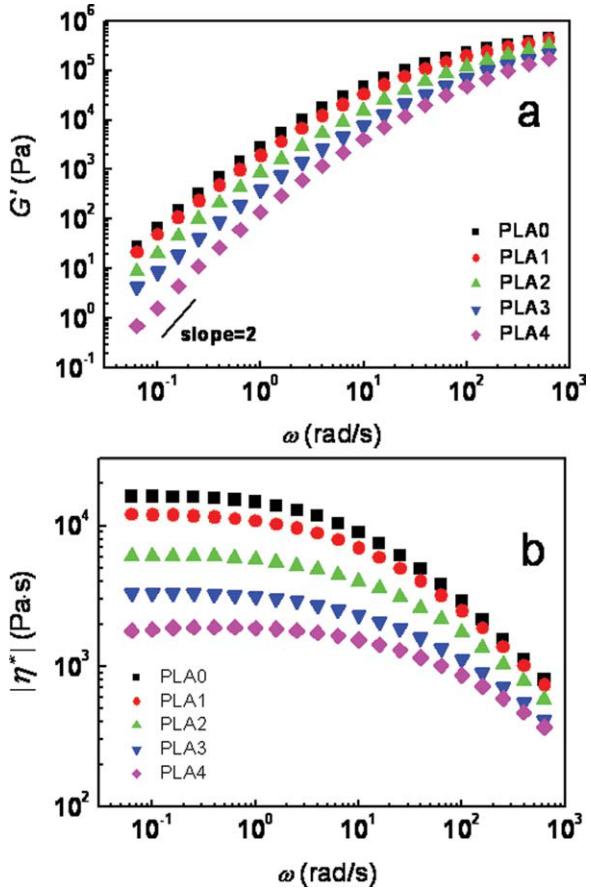

Figure 3 Variations of (a) storage modulus G' and (b) complex viscosity $|\eta^*|$ as functions of angular frequency ω at 160°C for PLA samples (PLA0 to PLA4). [Color figure can be viewed in the online issue, which is available at wileyonlinelibrary.com.]

enhanced, and the slopes obviously deviate from the terminal slope 2. Note that the global time for each frequency sweep is <2 h, thus this slope deviation from the terminal slope is irrespective to thermal stability of the samples. The increasing of G' and the declining of the slope of G' at the low frequency region are signatures of long-chain branched polymers.[12] The nonterminal behaviors for LCB-PLA1–4 suggest that a long relaxation mechanism exists in the low frequency region, which can be ascribed to LCB or slightly broad molecular mass distribution generated by free radical reactions. Addition of a low amount of TMPTA can effectively minimize degradation and simultaneously enhance chain fragments combination,[26] which introduces LCBs and consequently leads to the increasing of G'. In addition, LCB-PLA1–4 samples show slightly lower storage moduli than PLA0 in the high frequency region. This is not unexpected since a similar phenomenon was reported for branched polycarbonates[27] and poly butadiene/polyisoprene star/linear blend system,[28] although the explanation to this phenomenon remains an open issue. Figure 4(b) shows variations of complex viscosity $|\eta^*|$ or steady shear viscosity η as functions of frequency ω or shear rate $\dot{\gamma}$ for LCB-PLA1–4 at 160°C. According to the Cox–Merz rule,[29] the steady shear viscosity $\eta(\dot{\gamma})$ is

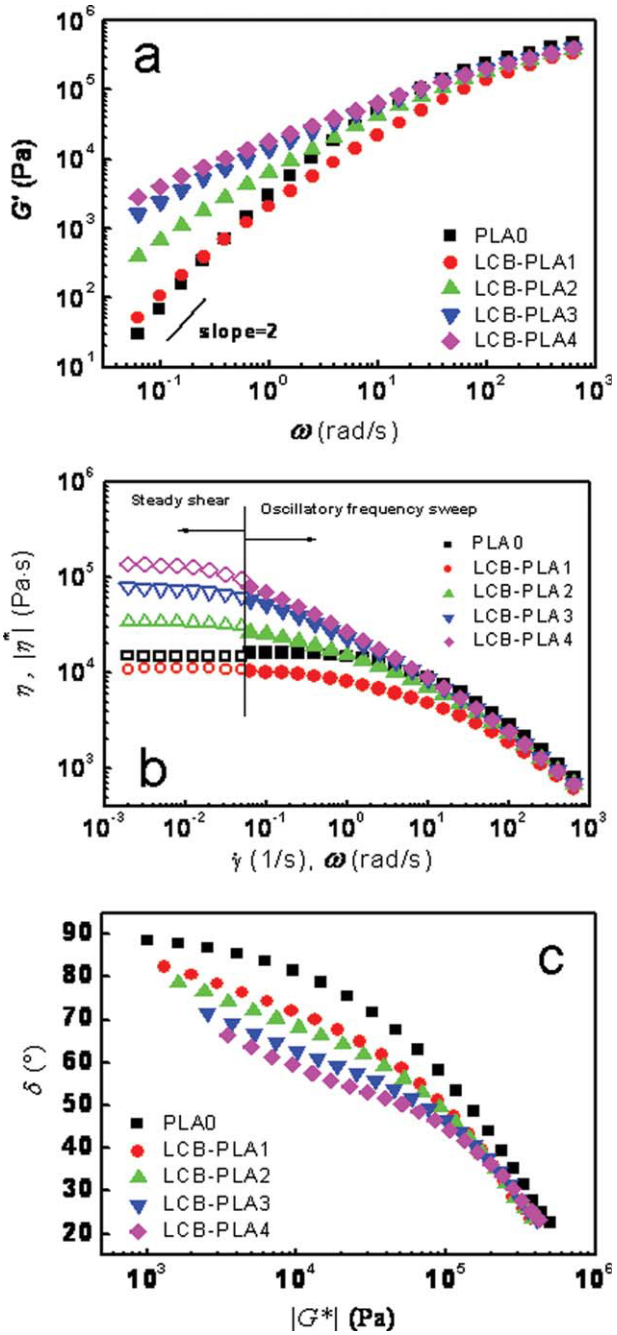

Figure 4 Variations of (a) storage modulus G' as functions of angular frequency ω, (b) steady shear viscosity η (open symbols) or complex viscosity $|\eta^*|$ (solid symbols) as functions of shear rate $\dot{\gamma}$ or angular frequency ω, and (c) the van Gurp–Palmen plots for PLA samples (LCB-PLA1–4) at 160°C. The data for PLA0 are also shown for comparison purpose. [Color figure can be viewed in the online issue, which is available at wileyonlinelibrary.com.]

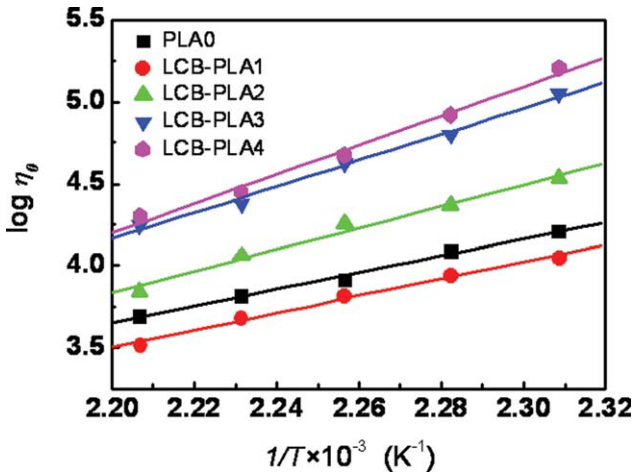

Figure 5 Temperature dependences of the zero shear viscosity η_0 for PLA samples (LCB-PLA1–4). The data for PLA0 are also shown for comparison purpose. [Color figure can be viewed in the online issue, which is available at wileyonlinelibrary.com.]

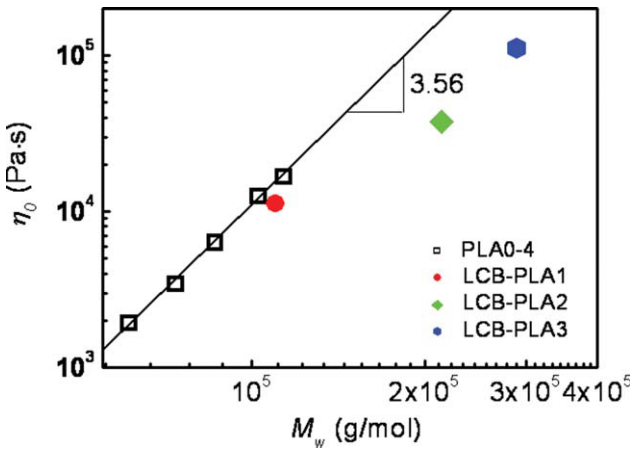

Figure 6 Variations of the zero shear viscosity η_0 at 160°C with mass average molecular mass M_w for the linear PLA samples (with no addition of TMPTA) and the branched PLA samples (with addition of varying amounts of TMPTA). [Color figure can be viewed in the online issue, which is available at wileyonlinelibrary.com.]

approximately equal to the complex viscosity $|\eta^*(\omega)|$ for sufficiently low shear rates, which can be expressed as $\lim_{\dot{\gamma}\to 0}\eta(\dot{\gamma}) = \lim_{\omega\to 0}|\eta^*(\omega)|$. By this principle, $\eta(\dot{\gamma})$ in the lower shear rate region can be combined with $|\eta^*(\omega)|$; hence, the Newtonian plateau can be broadly spanned down to almost 10^{-3} s^{-1}. $|\eta^*|$ [or $\eta(\dot{\gamma})$] values are greatly enhanced with increasing amount of TMPTA, which is consistent with G' evolutions. However, $|\eta^*|$ [or $\eta(\dot{\gamma})$] values of LCB-PLA1 are slightly lower than that of PLA0, which is due to irradiation-induced degradation and low amount of added TMPTA. The van Gurp–Palmen plots [Fig. 4(c)] can sensitively distinguish the LCB behaviors of polymers.[30,31] The loss angle δ is nearly 90° at the low values of $|G^*|$ for linear PLA0, which resembles that of linear polyethylenes. On the contrary, evident deviations are found for LCB-PLA1–4 samples. The deviation becomes more prominent with increasing TMPTA amount indicating enhanced LCB generation. It should be mentioned that the molecular mass distribution of polymers also affects phase difference in the van Gurp–Palmen plot; however, in this study the influence of LCB is dominant since the molecular mass distribution of LCB-PLA samples only shows slight changes (see Table II).

TABLE III
Apparent Flow Activation Energy, E_a^0, for PLA Samples

Sample code	E_a^0 (kJ/mol)
PLA0	42.4
LCB-PLA1	43.5
LCB-PLA2	54.8
LCB-PLA3	66.0
LCB-PLA4	74.2

Through combination of $\eta(\dot{\gamma})$ and $|\eta^*|$, the zero shear viscosity η_0 can be accurately obtained by fitting the data with the Cross model:

$$|\eta^*(\omega)| = \frac{\eta_0}{1 + (\tau\omega)^{1-n}}, \quad (1)$$

where τ is the characteristic relaxation time and its reciprocal accounts for onset of the shear thinning region, and n is an exponent. Figure 5 shows variations of η_0 versus $1/T$ for LCB-PLA1–4, which can be well fitted by using the Arrhenius equation as follows:

$$|\eta_0| = A\exp(E_a^0/RT), \quad (2)$$

where R is the gas constant, A is a constant, and E_a^0 is the flow activation energy. E_a^0 for each PLA sample can be determined, which is an important parameter to characterize the LCBs,[11,31,32] since it is independent of molecular mass and molecular mass distribution under the condition that the molecular mass exceeds a minimum value closely corresponding to the entanglement molecular mass, M_e. The obtained values of E_a^0 are listed in Table III, which are slightly lower than the previously reported data.[33] Compared with the PLA0, dramatic increases of E_a^0 are seen for LCB-PLA1–4, which suggests that the LCB level increases with increasing amount of added TMPTA. Note that the increasing of E_a^0 can be attributed to the branched structures, including either short-chain branches (SCBs) or LCBs. Therefore, further evidences from extensional rheological measurements are needed to verify the existence of LCB in LCB-PLA1–4.

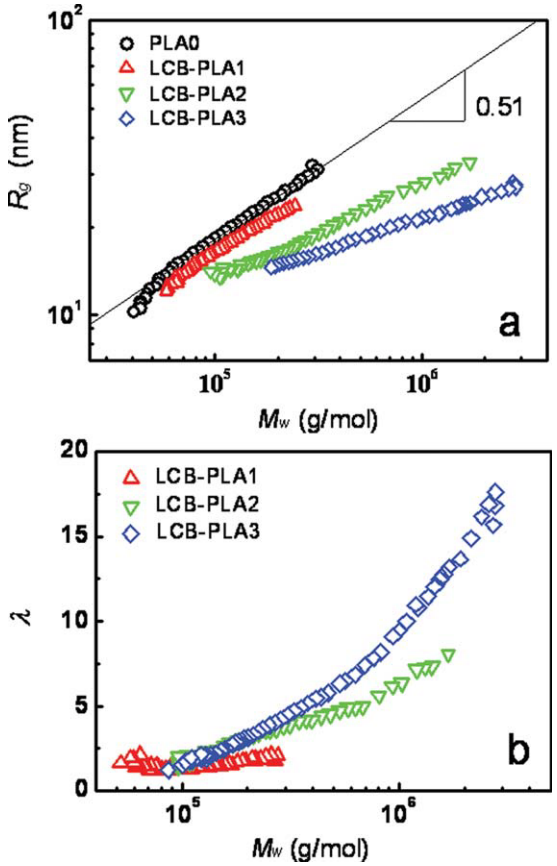

Figure 7 Variations of (a) the root mean square radius of gyration R_g and (b) the number of branches per 1000 monomer units λ as functions of mass average molecular mass M_w determined by SEC-MALLS measurements for PLA samples. [Color figure can be viewed in the online issue, which is available at wileyonlinelibrary.com.]

Determinations of PLA chain structures

Figure 6 shows the molecular mass dependence of η_0 for linear and branched PLA samples. The relation between η_0 and M_w is expected to follow Eq. (3) for linear polymers with molecular mass far beyond the critical molecular mass, M_c ($M_c = 2M_e$), where M_e refers to the entanglement molecular mass.

$$\log \eta_0 = A + 3.4 \log M_w \,(\text{for } M_w < M_c). \tag{3}$$

According to Ref. 8, M_e of PLA is about 4 kg mol^{-1}, which is much less than the mass average molecular mass (M_w) of the PLA samples used in this work. Therefore, the scaling relation in Eq. (3) should be obtained. By fitting the data of logη_0 and logM_w of the four PLA samples (PLA0, PLA1, PLA3, and PLA4), the power law dependence is obtained with an exponent of 3.56, which is approximately close to the generally regarded value of 3.4 and is also consistent with the previously reported value.[8] The earlier result indicates that the topology for the above four PLA samples remains linear, which further confirms our rheological results.

The relationship between η_0 and M_w is represented by a straight line for the linear PLA samples in Figure 6, while obvious deviations from the straight line are found for the three branched PLA samples. The data points beneath the straight line or a strong deviation toward lower η_0 can be designated to a tree-like branching topology, which is generally found for LDPE,[34,35] whereas an improvement of η_0 to above the straight line is typical for a slightly LCB polymer with a star-like or comb-like chain structure.[11,32,36] In addition, a tree-like chain structure has a high degree of branches with low arm molecular mass, whereas a comb-like chain structure has a low degree of branches with rather high arm molecular mass. Taking these into consideration, one can draw a conclusion according to Figure 6 that linear chains are apparent for PLA0 to PLA4 samples, and a tree-like chain structure is more possible for LCB-PLA1 to LCB-PLA3 samples.

To gain further insight into the PLA structures, variations of the root mean square radius of gyration, R_g, as a function of molecular mass M_w for both linear and branched PLA samples are shown in Figure 7(a). For most of linear viscoelastic polymers, the relationship between R_g and M_w can be well expressed by a power law written as follows:

$$R_g = KM_w^{\alpha}. \tag{4}$$

The slope α in Eq. (4) makes it possible to distinguish between linear and branched polymer chains. In our study, a slope of 0.51 is obtained for PLA0 (fitted by the solid line), which is a typical value for a random coil in a solvent and close to the theoretical exponent of 0.58.[37] It is interesting to find that reduction in R_g at a fixed M_w becomes more pronounced with increasing amount of added TMPTA (from LCB-PLA1 to LCB-PLA3). The slopes for branched PLA samples are 0.43, 0.34, and 0.23, respectively, implying increasing LCB levels. The number of branches per 1000 monomer units, λ, can be calculated according to the Zimm theory.[38]

$$g_M = \frac{\langle R_g^2 \rangle_{\text{br}}}{\langle R_g^2 \rangle_l} \tag{5}$$

$$g_M = \left[\left(1 + \frac{B_{3n}}{7} \right)^{0.5} + \frac{4B_{3n}}{9\pi} \right]^{-0.5} \tag{6}$$

$$\lambda = \frac{B_{3n}}{M} \times 1000 \times M_M. \tag{7}$$

In Eq. (5), g_M represents the branch index, and $\langle R_g^2 \rangle_{\text{br}}$ and $\langle R_g^2 \rangle_l$ are the mean square radii of gyration for branched and linear PLA chains, respectively. In Eq. (6), B_{3n} is the number of branching

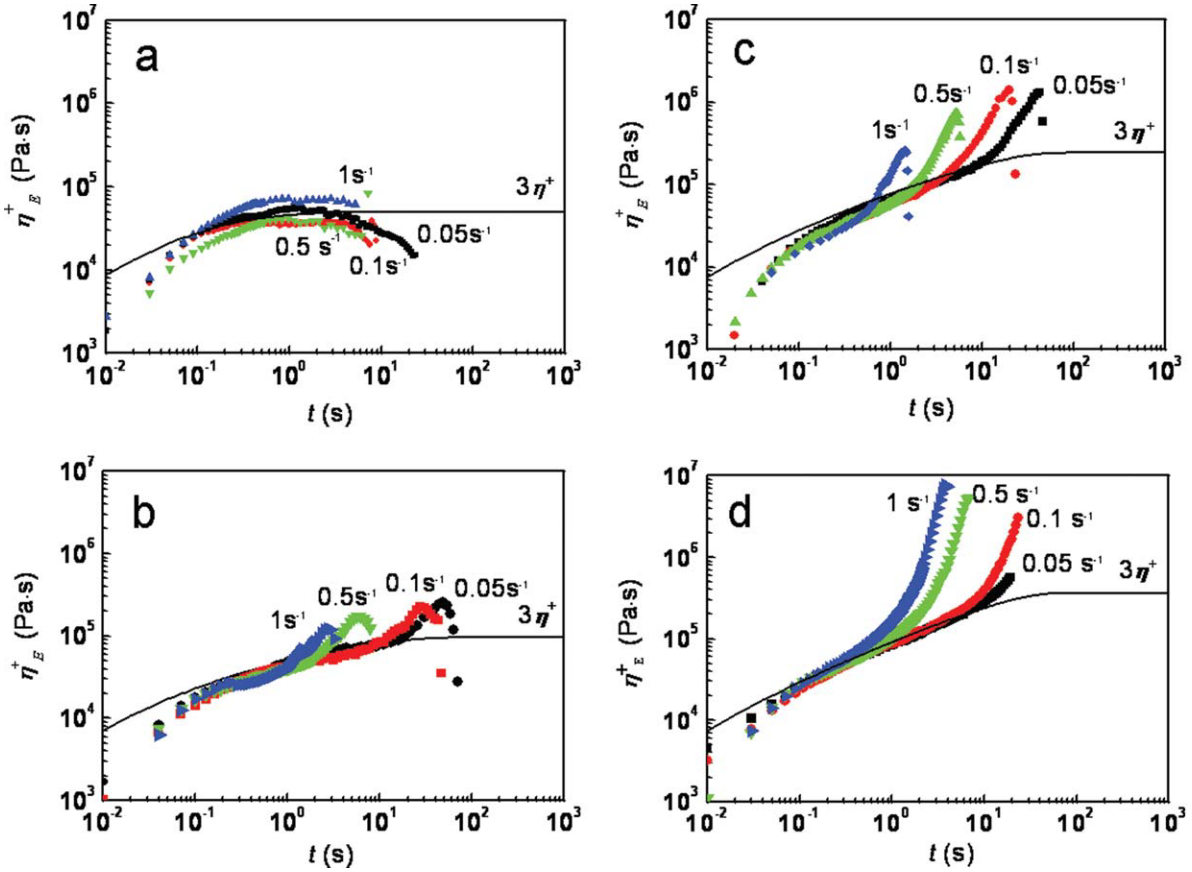

Figure 8 Variations of uniaxial extensional viscosity η_E^+ as functions of time t with different extensional rates at 160°C for (a) linear PLA sample, PLA0, and branched PLA samples, (b) LCB-PLA1, (c) LCB-PLA3, and (d) LCB-PLA4. [Color figure can be viewed in the online issue, which is available at wileyonlinelibrary.com.]

points per chain for three-arm-branched polymer. Since the branched PLA was prepared in presence of the trifunctional monomer TMPTA, Eq. (6) can be used to determine the number of branching points per chain, B_{3n}. In Eq. (7), M represents the molecular mass of branched PLA, and M_M is the molecular mass of the monomer unit, which is 72 g mol^{-1} for PLA.

The variations of λ versus M_w for branched PLA samples (LCB-PLA1 to LCB-PLA3) are shown in Figure 7(b). For LCB-PLA1, λ increases from around 1.2 to 2.5 in the measurable molecular mass range. This result demonstrates that LCB-PLA1 is sparsely branched. Furthermore, λ increases with increasing amount of TMPTA (from LCB-PLA1 to LCB-PLA3). It is expected that LCB-PLA3 can have a high degree of branches, which is evidenced by its λ values reaching up to 18 in the high molecular mass region. λ is of molecular mass dependence. Obviously, the high molecular mass component shows a high degree of branches. Thus, the data derived from the SEC-MALLS measurements not only convince the existence of branched structures for LCB-PLA samples but also can be used to determine the branch densities quantitatively.

Extensional rheological behaviors

It is well known from the literature that the time dependence of the extensional viscosity measured at constant strain rate can be affected by introducing a low amount of LCBs [34,39,40] despite some difficulties in the experimental procedure. Figure 8 shows the time-dependent extensional viscosities of PLA samples irradiated with addition of various amounts of TMPTA, which is approximately equal to the threefold of the time-dependent shear viscosity at all the experimentally accessible time and extensional rates. The strain-hardening behavior cannot be observed for the linear PLA sample (PLA0) shown in Figure 8(a); in contrast, it can be obviously observed for the branched PLA samples (LCB-PLA1, LCB-PLA3, and LCB-PLA4) shown in Figure 8(b–d), respectively, for which the transient extensional viscosity rises above three times of the linear viscoelastic start-up curve. Strain-hardening is obviously enhanced and of strong extensional rate dependence with increasing amount of TMPTA, which infers that LCB-PLA1 has a sparsely branched structure similar to mLLDPE,[34] and LCB-PLA3 and LCB-PLA4 have high amounts of LCB chain structures because of the increased

amounts of added TMPTA. The earlier results agree well with the chain structure changes concluded from the shear rheology and SEC-MALLS measurements. Moreover, for the PLA samples, the linear viscoelastic flow curves in extension correspond well to the threefold of the time-dependent shear viscosity as expected for a reliable measurement.

It should be mentioned that the extensional viscosity is reported to be affected also by the molecular mass distribution.[41] For example, blending a linear polymer with another linear polymer with ultrahigh molecular mass,[42] or with a crosslinked component,[43,44] can inspire a strain-hardening behavior. Therefore, the success of extensional rheology experiments on the branched PLA samples is based on the condition that the polydispersity (M_w/M_n) does not change much. In light of the molecular mass characterization, high molecular mass tails are not observed for the PLA samples, which means the effects from high molecular mass tails or a low amount of crosslinked component can be excluded. Thus, the strain-hardening behaviors in the extensional shear flow for the PLA samples are related to the long-chain branched structures.

CONCLUSIONS

Chain structure diversification of a series of PLA samples prepared by electron beam irradiation without or with addition of various amounts of a trifunctional monomer, TMPTA, was investigated by means of size-exclusion chromatography coupled with a light scattering detector (SEC-MALLS), shear, and extensional rheology. Without addition of TMPTA, the increasing irradiation dose enhances PLA degradation, while PLA chain structures remain linear. With addition of low amounts of TMPTA and electron beam irradiation, long-chain branched structures were successfully introduced into PLA samples, which show prominent higher zero shear viscosity, longer characteristic relaxation time, higher apparent flow activation energy, and pronounced strain-hardening behavior with extensional rate dependence. With increasing amount of TMPTA, the relation between R_g and M_w obviously deviates from the scaling relation for linear PLA samples, which strongly indicates the increased LCB degree for the branched PLA samples.

References

1. Tanaka, Y.; Yamaoka, H.; Nishizawa, S.; Nagata, S.; Ogasawara, T.; Asawa, Y.; Fujihara, Y.; Takato, T.; Hoshi, K. Biomaterials 2010, 31, 4506.
2. Moriya, A.; Maruyama, T.; Ohmukai, Y.; Sotani, T.; Matsuyama, H. J Membr Sci 2009, 342, 307.
3. Lindblad, M. S.; Liu, Y.; Albertsson, A. C.; Ranucci, E.; Karlsson, S. Adv Polym Sci 2002, 157, 139.
4. Lima, L. T.; Aurasb, R.; Rubino, M. Prog Polym Sci 2008, 33, 820.
5. Yan, D.; Wang, W. J.; Zhu, S. Polymer 1999, 40, 1737.
6. Agarwal, P. K.; Somani, R. H.; Weng, W. Q.; Mehta, A.; Yang, L.; Ran, S. F.; Liu, L. Z.; Hsiao, B. S. Macromolecules 2003, 36, 5226.
7. Fetters, L. J.; Lohse, D. J.; Milner, S. T.; Graessley, W. W. Macromolecules 1999, 32, 6847.
8. Dorgan, J. R.; Janzen, J.; Clayton, M. P. J Rheol 2005, 49, 607.
9. Malmberg, A.; Kokko, E.; Lehmus, P.; Lofgren, B.; Seppala, J. V. Macromolecules 1998, 31, 8448.
10. Krause, B.; Stephan, M.; Volkland, S.; Voigt, D.; Haüßler, L.; Dorschner, H. J Appl Polym Sci 2006, 99, 260.
11. Auhl, D.; Stange, J.; Münstedt, H.; Krause, B.; Voigt, D.; Lederer, A.; Lappan, U.; Lunkwitz, K. Macromolecules 2004, 37, 9465.
12. Wood-Adams, P. M.; Dealy, J. M.; deGroot, A. W.; Redwine, O. D. Macromolecules 2000, 33, 7489.
13. Wood-Adams, P. M.; Dealy, J. M. Macromolecules 2000, 33, 7481.
14. Stadler, F. J.; Piel, C.; Klimke, K.; Kaschta, J.; Parkinson, M.; Wilhelm, M.; Kaminsky, W.; Münstedt, H. Macromolecules 2006, 39, 1474.
15. Malmberg, A.; Liimatta, J.; Lehtinen, A.; Lofgren, B. Macromolecules 1999, 32, 6687.
16. Lohse, D. J.; Milner, S. T.; Fetters, L. J.; Xenidou, M.; Hadjichristidis, N.; Mendelson, R. A.; Garcia-Franco, C. A.; Lyon, M. K. Macromolecules 2002, 35, 3066.
17. Vega, J. F.; Santamaria, A.; Munõz-Escalona, A.; Lafuente, P. Macromolecules 1998, 31, 3639.
18. van Gurp, M.; Palmen, J. Rheol Bull 1998, 67, 5.
19. Hingmann, R.; Marczinke, B. L. J Rheol 1994, 38, 573.
20. Langston, J. A.; Colby, R. H.; Chung, T. C. M.; Shimizu, F.; Suzuki, T.; Aoki, M. Macromolecules 2007, 40, 2712.
21. Cooper-White, J. J.; Mackay, M. M. J Polym Sci Polym Phys 1999, 37, 1803.
22. Palade, L.; Lehermeier, H. J.; Dorgan, J. R. Macromolecules 2001, 34, 1384.
23. Dorgan, J. R.; Williams, J. S.; Lewis, D. N. J Rheol 1999, 43, 1141.
24. Dorgan, J. R.; Lehermeier, H.; Mang, M. J Polym Environ 2000, 8, 1.
25. Yamane, H.; Sasai, K.; Takano, M.; Takahashi, M. J Rheol 2004, 48, 599.
26. Yoshii, F.; Makuuchi, K.; Kikukawa, S.; Tanaka, T.; Saitoh, J.; Koyama, K. J Appl Polym Sci 1996, 60, 617.
27. Liu, C. Y.; Li, C. X.; Chen, P.; He, J. S.; Fan, Q. R. Polymer 2004, 45, 2803.
28. Milner, S. T.; McLeish, T. C. B.; Young, R. N.; Hakiki, A.; Johnson, J. M. Macromolecules 1998, 31, 9345.
29. Cox, W. P.; Merz, E. H. J Polym Sci 1958, 281, 619.
30. Vega, J. F.; Fernández1, M.; Santamaría, A.; Munñz-Escalona, A.; Lafuente, P. Macromol Chem Phys 1999, 200, 2257.
31. Stadler, F. J.; Kaschta, J.; Münstedt, H. Macromolecules 2008, 41, 1328.
32. Stange, J.; Wachter, S.; Münstedt, H.; Kaspar, H. Macromolecules 2007, 40, 2409.
33. Lehermeier, H. J.; Dorgan, J. R. Polym Eng Sci 2001, 41, 2172.
34. Stange, J.; Münstedt, H. J Rheol 2006, 50, 907.
35. Gabriel, C.; Münstedt, H. J Rheol 2003, 47, 619.
36. Stadler, F. J.; Nishioka, A.; Stange, J.; Koyama, K.; Münstedt, H. Rheol Acta 2007, 46, 1003.
37. le Guillou, J. C.; Zinn-Justin, J. Phys Rev Lett 1977, 39, 95.
38. Zimm, B. H.; Stockmayer, W. H. J Chem Phys 1949, 17, 1301.
39. Delgadillo-Velázquez, O.; Hatzikiriakos, S. G.; Sentmanat, M. J Polym Sci Part B: Polym Phys 2008, 46, 1669.
40. Delgadillo-Velázquez, O.; Hatzikiriakos, S. G.; Sentmanat, M. Rheol Acta 2008, 47, 19.
41. Hatzikiriakos, S. G. Polym Eng Sci 2000, 40, 2279.
42. Sugimoto, M.; Masubuchi, Y.; Takimoto, J.; Koyama, K. Macromolecules 2001, 34, 6056.
43. Yamaguchi, M. J Polym Sci Part B: Polym Phys 2001, 39, 228.
44. Yamaguchi, M.; Suzuki, K. J Appl Polym Sci 2002, 86, 79.